DRL-AdaPart: DRL-Driven Adaptive STAR-RIS Partitioning for Fair and Frugal Resource Utilization

Ashok S. Kumar, *Member, IEEE*, Nancy Nayak, *Member, IEEE*, Sheetal Kalyani, *Senior Member, IEEE*, and Himal A. Suraweera, *Senior Member, IEEE*

Abstract

In this work, we propose a method for efficient resource utilization of simultaneously transmitting and reflecting reconfigurable intelligent surface (STAR-RIS) elements to ensure fair and high data rates. We introduce a subsurface assignment variable that determines the number of STAR-RIS elements allocated to each user and maximizes the sum of the data rates by jointly optimizing the phase shifts of the STAR-RIS and the subsurface assignment variables using an appropriately tailored deep reinforcement learning (DRL) algorithm. The proposed DRL method is also compared with a Dinkelbach algorithm and the designed hybrid DRL approach. A penalty term is incorporated into the DRL model to enhance resource utilization by intelligently deactivating STAR-RIS elements when not required. The proposed DRL method can achieve fair and high data rates for static and mobile users while ensuring efficient resource utilization through extensive simulations. Using the proposed DRL method, up to 27% and 21% of STAR-RIS elements can be deactivated in static and mobile scenarios, respectively, without affecting performance.

Index Terms

Simultaneously transmitting and reflecting reconfigurable intelligent surfaces, deep reinforcement learning, resource utilization, user fairness.

A. S Kumar, and S. Kalyani are with the Department of Electrical Engineering, Indian Institute of Technology Madras, Chennai, India (e-mail: {ee22d023@smail, ee17d408@smail, skalyani@ee}.iitm.ac.in).

Nancy Nayak is with the Department of Electrical and Electronic Engineering, Imperial College London, United Kingdom (e-mail: n.nayak@imperial.ac.uk).

H. A. Suraweera is with the Department of Electrical and Electronic Engineering, University of Peradeniya, Peraeniya 20400, Sri Lanka (e-mail: himal@eng.pdn.ac.lk).

I. Introduction

Conventionally, reconfigurable intelligent surfaces (RISs) enhance the propagation environment by intelligently reflecting incident signals; however, they inherently restrict communication to 180°, leading to potential coverage dead zones [1]. Addressing this limitation, the innovation of simultaneously transmitting and reflecting RIS (STAR-RIS) emerges as a transformative solution [2]. The STAR-RIS can simultaneously reflect and transmit the incident signal, thus providing coverage to 360°, unlike traditional RIS, which can only reflect [3]–[5]. The STAR-RIS can be operated in one of the three practical modes, namely energy splitting (ES), mode switching (MS), and time switching (TS) [2], [3]. The MS mode is preferred in practice among these three protocols due to its ease of hardware implementation. The ES protocol involves optimizing more STAR-RIS coefficients, which increases computational complexity [6]. In addition, the ES protocol is restricted by the transmission-reflection phase correlation constraint, which leads to performance degradation [2], [3], [6]. However, the MS protocol is not restricted by such correlation, and hence, in this work, we consider the MS protocol for operating STAR-RIS.

The efficient utilization of resources in STAR-RIS is crucial in practical scenarios as it reduces power consumption, minimizes operational costs, and ensures reliable communication [7], [8]. Most of the existing work discusses the allocation of resources of STAR-RIS in terms of power, beamforming, channel, and time allocation [8]-[10]. In [8], the authors explore resource allocation in STAR-RIS in terms of channel assignment, power allocation, and beamforming to maximize sum rate for orthogonal multiple access, while also refining decoding order, beamforming vector, and power allocation for non-orthogonal multiple access. The work in [9] performs resource allocation by jointly optimizing time allocation and power allocation using a method based on Genetic algorithms to maximize total throughput. The authors in [10] aim to optimize resource allocation in terms of time, power, and data offloading in a mobile edge computing system aided by a STAR-RIS to iteratively minimize total energy consumption. To the best of our knowledge, none of the previous work delves into the fact that each user does not need to be allocated the same number of STAR-RIS elements in order to achieve a high and fair data rate. In this work, we determine the required number of STAR-RIS elements per user to achieve a fair and high data rate among all users. We refer to this quantity as the subsurface assignment variable, which indicates how many STAR-RIS elements should be assigned to serve each of the users to ensure fair data rates.

The first part of our work aims to maximize the data rates by jointly optimizing the phase shifts of the STAR-RIS and the subsurface assignment variable in the static user scenario. The authors in [11] and [12] discuss a multi-user STAR-RIS setup, in which the elements of the STAR-RIS have been partitioned equally into subsurfaces so that the system resources can be utilized more effectively. Equal partitioning of the STAR-RIS allots an equal number of elements to all the users. However, an equal partitioning of the STAR-RIS elements may result in resource over-utilization or under-utilization as users located closer to the STAR-RIS require fewer elements compared to those at greater distances. This observation motivates the proposal of an unequal partitioning strategy for the STAR-RIS to enhance resource utilization efficiency. By allocating more elements to distant users, their data rates can be improved, while assigning fewer elements to nearby users allows better utilization of STAR-RIS elements. In summary, a well-designed unequal partitioning scheme enhances the efficient utilization of STAR-RIS elements while ensuring fair data rates among users. This work examines the impact of both equal and unequal partitioning, particularly in a multi-user scenario.

TABLE I: Comparison of our work with state-of-the-art STAR-RIS communication systems.

Reference	BS-UE link	Channel (between STAR-RIS and BS)	Multi users	Static users	Mobile users	Partitioning of STAR-RIS elements	Exploring subsurface assignment variable for fair data rates	Selective deactivation of STAR-RIS elements
[11] [13], 2022	X	Rayleigh	1	✓	X	Equal	×	×
[14], 2023	Х	Nakagami	2 users	1	Х	Equal	Х	Х
[15], 2023	✓	Nakagami	1	1	×	None	×	X
[16], 2024	X	Rician	1	1	×	None	×	×
[17]–[19], 2024	1	Rician	1	1	х	None	Х	Х
[20], 2024	✓	Rician	1	X	1	None	×	×
[21], 2025	х	Rayleigh	2 users	Х	1	Equal	Х	Х
Our work	1	Rician	1	1	1	Equal and Unequal	1	√

The works reported in [22]-[24] use traditional optimization algorithms to solve the

non-convex optimization problem of finding the phase shifts of the RIS and beamformers at the base station (BS). The complexity of such algorithms increases with both unknown communication scenarios and with an increasing number of users and STAR-RIS elements [23]. Deep reinforcement learning (DRL) can solve such complex, high-dimensional problems by formulating them as a Markov decision process (MDP). Many works explore the advantage of the DRL approach in RIS for predicting the phase shifts of the RIS, active beamformers at the BS [19], [25], [26], maximizing the weighted sum rate of uplink (UL) and downlink (DL) users, and maximizing coverage and capacity [27]. Given that the issue with the subsurface assignment variable is inherently a combinatorial problem, we are inspired to exploit the power of DRL to solve both the phase shifts of the STAR-RIS and the subsurface assignment variables.

The authors of [28] and [29] consider the scenario of moving users, in which they propose an RIS-assisted system that handles users' mobility. In the context of mobile users, equal partitioning falls short due to its inability to adapt to the diverse needs of each user. However, unequal partitioning allows dynamic allocation of the STAR-RIS elements effectively, with varying user demands. Thus, unequal partitioning of STAR-RIS elements is more effective in mobile scenarios than equal partitioning. In mobile user scenarios, the traditional optimization algorithm faces even greater challenges in optimizing the phase shifts of the RIS and beamformers at the BS as the channel characteristics change over time [26]. Our proposed DRL approach can work well in both static and mobile scenarios.

We also investigated the effect of selective deactivation of the STAR-RIS elements on our system's performance. We believe that by adopting the selective deactivation of STAR-RIS elements, the overall power consumption of the system can be reduced, and the system can further improve the resource utilization of STAR-RIS elements. Thus, the DRL algorithm helps the STAR-RIS make real-time decisions about the deactivation of elements, enhancing resource utilization and performance. In Table I, we compare our work with the existing literature on STAR-RIS communication systems.

The main contributions of our work are summarized as follows:

• We propose a novel technique to achieve fair and high data rates for static and mobile users by efficiently utilizing the STAR-RIS elements in multi-user STAR-RIS DL scenarios. To achieve this objective, we introduce a new parameter, namely the subsurface assignment variable, which determines how many elements of STAR-RIS are allotted to a particular downlink user (DU). This variable enhances the flexibility of the STAR-RIS elements to

provide balanced data rates, thereby improving fairness among the DUs.

- We formulate a joint optimization problem that optimizes the phase shift of the STAR-RIS
 and the subsurface assignment variable, and then propose to solve it using an appropriately
 designed DRL technique.
- We further propose the possibility of selective deactivation of STAR-RIS elements to enhance resource utilization without affecting the individual data rates of each DU.
- Our technique remains effective even in the presence of mobile DUs, where the channel condition of the DUs keeps changing as they move, and the system becomes highly dynamic.
- We devised two different ways to compare the proposed DRL method. We compared the proposed DRL method with an existing conventional scheme called Dinkelbach that solves for STAR-RIS phase shifts. The DRL method achieves a 52% higher average DL data rate compared to the Dinkelbach algorithm. We have been further motivated to propose a hybrid approach in which the STAR-RIS phase shifts are optimized using the Dinkelbach algorithm, and binary subsurface assignment variables are optimized using the DRL method iteratively, and compare this with the proposed DRL method. The proposed DRL method is observed to perform 46% better than the hybrid DRL approach.

The rest of the paper is organized as follows. Section II presents the system model for the multi-user STAR-RIS system. We detail the proposed approach in Sections III and IV. Section V provides the simulation results, followed by conclusions in Section VI.

Notation: Scalars are represented in lowercase, while vectors and matrices are denoted by lowercase bold and uppercase bold, respectively. The transpose and conjugate transpose of a vector or matrix are denoted by $(.)^T$ and $(.)^H$, respectively. Also, diag represent the diagonal matrix and $\|.\|$ represents the Euclidean norm. \mathbb{C} and \mathbb{R} represent complex and real sets of numbers, respectively.

II. SYSTEM MODEL

Consider a scenario of STAR-RIS assisted DL transmission as depicted in Fig. 1. The BS has a uniform linear antenna consisting of M transmit antennas. Due to blockages, direct links between BS and DUs are assumed to be weak. Therefore, the BS communicates with the DUs with the assistance of a STAR-RIS. The STAR-RIS consists of $N = N^h N^v$ elements arranged in a uniform planar array with N^h horizontal and N^v vertical elements. The reflected signal from STAR-RIS remains in the same region as the incident wave (reflection space), while the

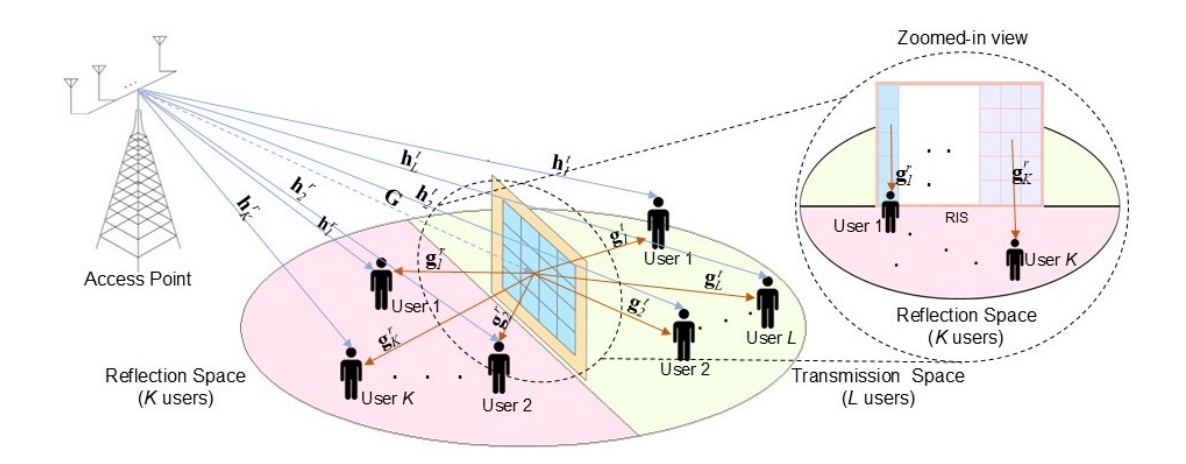


Fig. 1: Proposed system model for multi-user STAR-RIS system with partitioning. We have K users in the reflection space and L users in the transmission space. The zoomed-in view illustrates the partitioning of the N element STAR-RIS. User one, being closer, is allocated fewer elements, while user K, being farther, is allocated more elements.

transmitted signal propagates into the other region of STAR-RIS (transmission space) [3]. There are K DUs in the reflection space and L DUs in the transmission space such that K+L=J< N. Let P_t be the transmit power of the BS. Assuming equal power allocation among the J DUs, the transmit power allocated to each DU is $\rho_t = \frac{P_t}{J}$ [30]. Let x_j be the data symbol intended for the j^{th} DU such that $\mathbb{E}\{|x_j|^2\}=1, \ \forall j\in\{1,2,\ldots,J\}$ [18]. The channel between BS and STAR-RIS is given by $\mathbf{G}\in\mathbb{C}^{N\times M}$. The channel between STAR-RIS and k-th (l-th) DU in the reflection (transmission) space is given by $\mathbf{g}_k^r\in\mathbb{C}^{1\times N}$ ($\mathbf{g}_l^t\in\mathbb{C}^{1\times N}$). The channel between BS and k-th (l-th) DU in the reflection (transmission) space is given by $\mathbf{h}_k^r\in\mathbb{C}^{1\times M}$ ($\mathbf{h}_l^t\in\mathbb{C}^{1\times M}$). The reflection and transmission coefficient matrices of STAR-RIS are given by $\mathbf{\Theta}^r$, $\mathbf{\Theta}^t\in\mathbb{C}^{N\times N}$ where

$$\Theta^{r} = \operatorname{diag}\left[\sqrt{\beta_{1}^{r}}e^{j\theta_{1}^{r}}, \cdots, \sqrt{\beta_{n}^{r}}e^{j\theta_{n}^{r}}, \cdots, \sqrt{\beta_{N}^{r}}e^{j\theta_{N}^{r}}\right]^{T}
\Theta^{t} = \operatorname{diag}\left[\sqrt{\beta_{1}^{t}}e^{j\theta_{1}^{t}}, \cdots, \sqrt{\beta_{n}^{t}}e^{j\theta_{n}^{t}}, \cdots, \sqrt{\beta_{N}^{t}}e^{j\theta_{N}^{t}}\right]^{T}.$$
(1)

We consider the MS protocol for the operation of STAR-RIS, where each element operates either in reflection mode or in transmission mode. For example, if the n-th element is allotted for a DU in the reflection space, then $\beta_n^r=1$ and $\beta_n^t=0$. Similarly, if the n-th element is allotted for a DU in the transmission space, then $\beta_n^t=1$ and $\beta_n^r=0$. Therefore, $\beta_n^r,\beta_n^t\in\{0,1\}$, $\beta_n^r+\beta_n^t=1$ and $\theta_n^r,\theta_n^t\in[0,2\pi)\forall n\in\{1,...,N\}$ which characterize the amplitude and phase modifications imposed on the reflected and transmitted signal components, respectively [3].

Let $\alpha_{kn}^r, \alpha_{ln}^t \in \{0,1\}$ be the STAR-RIS subsurface (element) assignment variables where $\alpha_{kn}^r = 1$ means that subsurface n is assigned to the k-th DU in the reflection space. For a specific element n, $\sum_{k=1}^K \alpha_{kn}^r + \sum_{l=1}^L \alpha_{ln}^t \leq 1$, indicating that each element of the STAR-RIS should be assigned to at most one DU. However, more than one element can be assigned to one DU. Hence, the subsurface assignment variable decides if a particular STAR-RIS element is allotted to a DU. The reflection and transmission coefficients for the k-th and the l-th DU in the reflection and transmission space after incorporating the subsurface assignment variables are $\tilde{\Theta}_k^r = \mathrm{diag}\left(\tilde{\mathbf{s}}_k^r\right)$, and $\tilde{\Theta}_l^t = \mathrm{diag}\left(\tilde{\mathbf{s}}_l^t\right)$ respectively, such that

$$\tilde{\mathbf{s}}_{k}^{r} = \left[\alpha_{k1}^{r} \sqrt{\beta_{1}^{r}} e^{j\theta_{1}^{r}}, \cdots, \alpha_{kn}^{r} \sqrt{\beta_{n}^{r}} e^{j\theta_{n}^{r}}, \cdots, \alpha_{kN}^{r} \sqrt{\beta_{N}^{r}} e^{j\theta_{N}^{r}} \right]^{T},
\tilde{\mathbf{s}}_{l}^{t} = \left[\alpha_{l1}^{t} \sqrt{\beta_{1}^{t}} e^{j\theta_{1}^{t}}, \cdots, \alpha_{ln}^{t} \sqrt{\beta_{n}^{t}} e^{j\theta_{n}^{t}}, \cdots, \alpha_{lN}^{t} \sqrt{\beta_{N}^{t}} e^{j\theta_{N}^{t}} \right]^{T}.$$
(2)

Since, according to MS protocol, each element can serve a DU in either reflection or transmission space, we represent the phase shift vector as

$$\psi = [e^{j\theta_1^{\{r,t\}}}, \dots, e^{j\theta_n^{\{r,t\}}}, \dots, e^{j\theta_N^{\{r,t\}}}].$$
(3)

The superscript $\{r,t\}$ indicates that the element serves a DU in the reflection or in the transmission space. We assume that N^r and N^t elements are operating in the reflection and the transmission mode, respectively [2] and, therefore, $N^t + N^r = N$. The subsurface assignment matrix is $\mathbf{A} = [\mathbf{A}^r, \mathbf{A}^t]^T \in \{0,1\}^{(K+L)\times N}$, where

$$\mathbf{A}^r = [\boldsymbol{\alpha}_1^r, \boldsymbol{\alpha}_2^r, \dots, \boldsymbol{\alpha}_K^r], \ \mathbf{A}^t = [\boldsymbol{\alpha}_1^t, \boldsymbol{\alpha}_2^t, \dots, \boldsymbol{\alpha}_L^t]$$
$$\boldsymbol{\alpha}_k^r = [\alpha_{k1}^r, \alpha_{k2}^r, \dots, \alpha_{kN}^r]^T, \ \boldsymbol{\alpha}_l^t = [\alpha_{l1}^t, \alpha_{l2}^t, \dots, \alpha_{lN}^t]^T$$
(4)

such that for a specific element n, $\sum_{k=1}^{K} \alpha_{kn}^r + \sum_{l=1}^{L} \alpha_{ln}^t \leq 1$. Let the transmitted signal from the BS is

$$\mathbf{x} = \sum_{j=1}^{J} \mathbf{w}_j x_j \sqrt{\rho_t}.$$
 (5)

Here, $\mathbf{w}_j \in \mathbb{C}^{M \times 1}$ represents the beamforming vector for the j-th DU [18], [19].

The total received signal at the k-th DU in the reflection space is

$$y_k = (\mathbf{g}_k^r \tilde{\mathbf{\Theta}}_k^r \mathbf{G} + \mathbf{h}_k^r) \mathbf{w}_k x_k \sqrt{\rho_t} + (\mathbf{g}_k^r \tilde{\mathbf{\Theta}}_k^r \mathbf{G} + \mathbf{h}_k^r) \sum_{\substack{j=1\\j \neq k}}^J \mathbf{w}_j x_j \sqrt{\rho_t} + n_k.$$
(6)

The received signal at the k-th DU comprises the desired signal, contributed by both the direct path from the BS and the reflection path via the STAR-RIS 1 . It also includes interference from all other DUs in both the transmission and reflection spaces. Similarly, the total received signal at the l-th DU in the transmission space is

$$y_{l} = (\mathbf{g}_{l}^{t}\tilde{\mathbf{\Theta}}_{l}^{t}\mathbf{G} + \mathbf{h}_{l}^{t})\mathbf{w}_{l}x_{l}\sqrt{\rho_{t}} + (\mathbf{g}_{l}^{t}\tilde{\mathbf{\Theta}}_{l}^{t}\mathbf{G} + \mathbf{h}_{l}^{t})\sum_{\substack{j=1\\j\neq l}}^{J}\mathbf{w}_{j}x_{j}\sqrt{\rho_{t}} + n_{l},$$
(7)

where $n_k \sim \mathcal{CN}(0, \sigma_k^2)$ and $n_l \sim \mathcal{CN}(0, \sigma_l^2)$ [3]. Here, n_k and n_l denote the additive white Gaussian noise at the k-th and l-th DU, respectively.

The signal-to-interference-plus-noise ratios (SINR) of the DUs denoted by γ is given by the concatenation of the SINRs, γ_r and γ_t , corresponding to DUs in the reflection space and transmission space, respectively, where $\gamma = [\gamma_r, \gamma_t], \ \gamma_r = [\gamma_1^r, \gamma_2^r, \dots, \gamma_K^r], \ \text{and} \ \gamma_t = [\gamma_1^t, \gamma_2^t, \dots, \gamma_L^t].$

Let, the SINR of DU k in the reflection space γ_k^r is given by

$$\gamma_k^r = \frac{\rho_t \|\mathbf{g}_k^r \tilde{\mathbf{\Theta}}_k^r \mathbf{G} \mathbf{w}_k + \mathbf{h}_k^r \mathbf{w}_k\|^2}{\sum\limits_{\substack{j=1\\j\neq k}}^J \rho_t \|\mathbf{g}_k^r \tilde{\mathbf{\Theta}}_k^r \mathbf{G} \mathbf{w}_j + \mathbf{h}_k^r \mathbf{w}_j\|^2 + \sigma_k^2}.$$
(8)

The SINR of DU l in the transmission space γ_l^t is given by

$$\gamma_l^t = \frac{\rho_t \|\mathbf{g}_l^t \tilde{\mathbf{\Theta}}_l^t \mathbf{G} \mathbf{w}_l + \mathbf{h}_l^t \mathbf{w}_l\|^2}{\sum\limits_{\substack{j=1\\i \neq l}} \rho_t \|\mathbf{g}_l^t \tilde{\mathbf{\Theta}}_l^t \mathbf{G} \mathbf{w}_j + \mathbf{h}_l^t \mathbf{w}_j\|^2 + \sigma_l^2}.$$
(9)

The objective is to maximize the sum of the data rates of all the DUs in both reflection and transmission spaces. The data rate r_k^r and r_l^t for the k-th DU and for the l-th DU, in the reflection space and transmission space, respectively, can be expressed as

$$r_k^r = \log_2(1 + \gamma_k^r),$$

$$r_l^t = \log_2(1 + \gamma_l^t).$$
(10)

¹This work assumes that the STAR-RIS achieves directional capability to serve specific DUs via subsurface allocation, where each partition is formed by multiple elements coordinated to steer reflected/transmitted beams [31]. Based on this, interference from unallocated elements is neglected in this work, but may be explored in future works.

A. Optimization objective

We aim to maximize the sum of the DU data rates so that all users are served well. We try to find the optimal subsurface assignment and the corresponding optimal phase shift. The optimization problem is framed as follows.

$$\mathcal{P}_1: \quad \max_{\boldsymbol{\psi}, \mathbf{A}} \qquad \sum_{k=1}^K r_k^r + \sum_{l=1}^L r_l^t$$
 (11a)

s.t.
$$0 \le \theta_n^{\{r,t\}} \le 2\pi \quad \forall n \in 1, 2, \dots, N$$
 (11b)

$$\sum_{n=1}^{N} \alpha_{kn}^{r} \ge 1 \quad \forall k \in 1, 2, \dots, K$$
 (11c)

$$\sum_{n=1}^{N} \alpha_{ln}^{t} \ge 1 \quad \forall l \in 1, 2, \dots, L$$
 (11d)

$$\sum_{k=1}^{K} \alpha_{kn}^{r} + \sum_{l=1}^{L} \alpha_{ln}^{t} \le 1 \quad \forall n \in 1, \dots, N$$
 (11e)

Recall that α_{kn}^r is the n-th subsurface assignment variable corresponding to k-th DU in the reflection space, and α_{ln}^t is the n-th subsurface assignment variable corresponding to l-th DU in the reflection space. It should be noted that $\sum_{n=1}^N \alpha_{kn}^r \geq 1$, which indicates that at least one subsurface must be assigned to the k-th DU in the reflection space. Similarly, $\sum_{n=1}^N \alpha_{ln}^t \geq 1$ indicates that at least one subsurface must be assigned to the l-th DU in the transmission space.

B. Design model for beamformers

Beamforming is a signal processing technique that directs the signals towards an intended direction while minimizing interference in other directions. In our work, we design beamformers \mathbf{w}_j , $\forall j \in J$, using two different schemes, maximum ratio transmission (MRT) and zero-forcing (ZF) techniques [25]. The MRT beamforming vectors \mathbf{w}_k and \mathbf{w}_l for the k-th and l-th DUs in the reflection and transmission space, respectively, are given by

$$\mathbf{w}_{k} = \frac{(\mathbf{g}_{k}^{r} \tilde{\mathbf{O}}_{k}^{r} \mathbf{G} + \mathbf{h}_{k}^{r})^{H}}{\|\mathbf{g}_{k}^{r} \tilde{\mathbf{O}}_{k}^{r} \mathbf{G} + \mathbf{h}_{k}^{r}\|}, \ \mathbf{w}_{l} = \frac{(\mathbf{g}_{l}^{t} \tilde{\mathbf{O}}_{l}^{t} \mathbf{G} + \mathbf{h}_{l}^{t})^{H}}{\|\mathbf{g}_{l}^{t} \tilde{\mathbf{O}}_{l}^{t} \mathbf{G} + \mathbf{h}_{l}^{t}\|}.$$
(12)

ZF beamforming is a key technique in multi-user communication systems, designed to eliminate inter-user interference by ensuring that the transmitted signals are orthogonal to the unintended user's channel vectors. Let $\mathbf{W} \in \mathbb{C}^{M \times J}$ denote the ZF beamforming matrix with column vectors $\mathbf{w}_1, \mathbf{w}_2, \dots, \mathbf{w}_J$ and $\mathbf{H} \in \mathbb{C}^{J \times M}$ represent the effective channel matrix. The

effective channel matrix $\mathbf{H} \in \mathbb{C}^{J \times M}$ comprises K rows corresponding to the DUs in the reflection space, each of the form $(\mathbf{g}_k^r \tilde{\mathbf{\Theta}}_k^r \mathbf{G} + \mathbf{h}_k^r)$ for the k-th DU, and L rows corresponding to the DUs in the transmission space, each of the form $(\mathbf{g}_l^t \tilde{\mathbf{\Theta}}_l^t \mathbf{G} + \mathbf{h}_l^t)$ for the l-th DU. The ZF beamforming matrix \mathbf{W} satisfies $\mathbf{H}\mathbf{W} = \mathbf{I}$, where \mathbf{I} is the identity matrix [32]. The beamforming vector \mathbf{w}_k for the k-th DU in the reflection space is computed as

$$\mathbf{w}_k = \mathbf{H}^H (\mathbf{H}\mathbf{H}^H)^{-1} \mathbf{e}_k, \tag{13}$$

and then normalized. Here, e_k is the standard basis vector corresponding to the k-th DU. A similar expression can also be derived for DUs in the transmission space. Our objective is to focus on optimizing the phase shift of the STAR-RIS and the subsurface assignment variable for efficient resource utilization, which are critical to achieving fair and high data rates for users in both static and dynamic environments. It is also feasible to optimize the beamformers, but that is outside the scope of our work.

C. Channel Model

The Rician channel models a wireless communication environment with a dominant line-of-sight (LoS) component along with multiple scattered multipath components. The channels between STAR-RIS and BS, STAR-RIS and users, and between BS and users are modeled according to Rician fading [33], [34]. The channel between the BS and the k-th DU in the reflection space can be modeled as [20]:

$$\mathbf{h}_{k}^{r} = \sqrt{PL_{k}^{b}} \left(\sqrt{\frac{\kappa_{d}}{\kappa_{d} + 1}} \mathbf{h}_{k}^{L} + \sqrt{\frac{1}{\kappa_{d} + 1}} \mathbf{h}_{k}^{NL} \right). \tag{14}$$

Here, $\mathbf{h}_k^{\mathrm{L}}$ and $\mathbf{h}_k^{\mathrm{NL}}$ represent the LoS and the non-LoS component of $\mathbf{h}_k^{\mathrm{r}}$. The LoS component $\mathbf{h}_k^{\mathrm{L}} \in \mathbb{C}^{1 \times M}$ is given by $\mathbf{h}_k^{\mathrm{L}} = e^{\jmath 2\pi \left(f_k^b\right)\tau_k^b}\mathbf{a}_B\left(\theta_k^b,\phi_k^b\right)$, where f_k^b is the Doppler frequency shift for $\mathbf{h}_k^{\mathrm{r}}$. The Doppler frequency shift is given by $f_k^b = v\cos\theta_k^b\cos\phi_k^b/\lambda$, where λ represents the wavelength. The antenna array response is given by $\mathbf{a}_B\left(\theta_k^b,\phi_k^b\right) = \left[1,\ldots,e^{-j\frac{2\pi}{\lambda}\hat{d}_a(M-1)\sin\left(\theta_k^b\right)\cos\left(\phi_k^b\right)}\right]$, where θ_k^b and ϕ_k^b are the azimuth and elevation angles, respectively. The distance between the antenna elements is given by \hat{d}_a . The non-LoS component, $\mathbf{h}_k^{\mathrm{NL}} \in \mathbb{C}^{1 \times M}$ can be modeled as a complex Gaussian random vector $\mathcal{CN}(0,I_M)$. The distance-dependent path loss is given by $PL_k^b = C_0d_k^{b^{-\zeta_k^b}}$, where $C_0 = (\frac{c}{4\pi f_c d_0})$ denotes the path loss at the reference distance $d_0 = 1$ m [27]. The carrier frequency is given by f_c , and c represents the speed of light. Here, $d_k^b = \|D_k - D_{\mathrm{BS}}\|$ and ζ_k^b represent the path loss exponent.

Note that D_k represents the location vector of the k-th DU and D_{BS} denotes the location vector of the BS. The delay in the direct link of the k-th DU can be calculated as $\tau_k^b = \frac{d_k^b}{c}$. In addition, κ_d represents the Rician factors for h_k^r . The channel between STAR-RIS and k-th DU in the reflection space can be modeled as [35]:

$$\mathbf{g}_k^r = \sqrt{PL_k^s} \left(\sqrt{\frac{\xi_d}{\xi_d + 1}} \mathbf{g}_k^{\mathrm{L}} + \sqrt{\frac{1}{\xi_d + 1}} \mathbf{g}_k \right). \tag{15}$$

Similarly, the channel between BS and STAR-RIS can be modeled as

$$G = \sqrt{PL_b^s} \left(\sqrt{\frac{\rho_d}{\rho_d + 1}} G^{\mathcal{L}} + \sqrt{\frac{1}{\rho_d + 1}} G^{\mathcal{NL}} \right). \tag{16}$$

The path loss components are given by $PL_k^s = C_0 d_k^{s^{-\zeta_k^s}}$ and $PL_b^s = C_0 d_b^{s^{-\zeta_k^s}}$, respectively [35]. Here $d_k^s = \|D_k - D_S\|$ and $d_b^s = \|D_S - D_{\rm BS}\|$. In addition, D_S denotes the location vector of the STAR-RIS. The LoS component $g_k^{\rm L}$ is given by $g_k^{\rm L} = e^{\jmath 2\pi \left(f_k^s\right)\tau_k^s} \mathbf{a}_R\left(\theta_k^s, \phi_k^s\right)$. The delay $\tau_k^s = \frac{d_k^s}{c}$. The antenna array response vectors of STAR-RIS are given by

$$\mathbf{a}_{R}\left(\theta_{k}^{s}, \phi_{k}^{s}\right) = \left[1, \dots, e^{-j\frac{2\pi}{\lambda}\hat{d}_{s}\left(N^{h}-1\right)\sin\left(\theta_{k}^{s}\right)\cos\left(\phi_{k}^{s}\right)}\right]$$

$$\otimes \left[1, \dots, e^{-j\frac{2\pi}{\lambda}\hat{d}_{s}\left(N^{v}-1\right)\sin\left(\theta_{k}^{s}\right)\cos\left(\phi_{k}^{s}\right)}\right],$$

where θ_k^s and ϕ_k^s are the azimuth and elevation angles. The separation distance between the STAR-RIS elements is \hat{d}_s . ξ_d denote the Rician factor components of g_k^r and $f_k^s = v\cos\theta_k^s\cos\phi_k^s/\lambda$ represents the Doppler shift for g_k^r . The influence of Doppler is not considered in the channel between BS and STAR-RIS since both are stationary. Therefore, G^L is given by $G^L = \mathbf{a}_R (\theta_b^s, \phi_b^s) \mathbf{a}_B^H (\theta_s^b, \phi_s^b)$, where $\theta_b^s (\theta_s^b)$ and $\phi_b^s (\phi_s^b)$ are the azimuth and elevation angles. In addition, ρ_d represents the Rician factor component of G. Also, note that $g_k^{\rm NL} \sim \mathcal{CN}(0, I_N)$, and $G^{\rm NL} \sim \mathcal{CN}(0, I_{NM})$. Similar expressions can also be derived for DUs within the transmission space. The path loss components in the channel from BS to STAR-RIS and from STAR-RIS to the DUs are $\zeta_b^s = \zeta_k^s = 2.2$ [36]. The same in the channel from the BS to the DU is $\zeta_k^b = 3.35$ [36].

III. DEEP REINFORCEMENT LEARNING-BASED RESOURCE UTILIZATION FOR ACHIEVING FAIR DATA RATES

The proposed optimization problem \mathcal{P}_1 in (11) maximizes the sum of the data rates of all DUs in both the reflection and transmission spaces. In addition, we propose a method to enhance resource utilization by selectively deactivating STAR-RIS elements. In both cases,

the optimization objective is non-convex with integer constraints on the subsurface assignment variable. A similar mixed-integer non-convex problem was addressed in [24], where the authors have converted it to a convex problem, by relaxing the binary constraint using a penalty-based approach and adding it to the objective function. Then it is solved using successive convex approximation, resulting in a suboptimal solution. This type of solution may not be appropriate if the channel conditions of the users vary a lot and the solution needs to be calculated at every timestep. In contrast to this, DRL algorithms do not need to relax the integer constraints and can handle high-dimensional and combinatorial optimization problems more effectively [37]–[39]. A mixed integer nonlinear programming (MINLP) problem for user scheduling, phase shift, and beamforming optimization is illustrated in [40], and DRL is shown to outperform alternating optimization in terms of both aggregated throughput and runtime. In this work, the non-convex integer constraint problem we address becomes non-stationary when the DUs are mobile, as it creates a dynamic environment where the positions and channel conditions of DUs constantly change. The proposed DRL algorithm can predict subsurface assignment variables based on the channel condition and how far the mobile DU is from STAR-RIS at every time step.

We model the problem of estimating the STAR-RIS phase shifts and subsurface assignment variables as an MDP with a state space (S), an action space (A), an initial state distribution $p(s^{\{1\}})$, a stationary state transition distribution following $p(s^{\{t'+1\}}|s^{\{t'\}},a^{\{t'\}}) =$ $p(s^{\{t'+1\}}|s^{\{t'\}},a^{\{t'\}},\dots,s^{\{1\}},a^{\{1\}}))$ adhering to the Markov property [33], [41]. Here, the superscript t' indicates the values at the time step t'. The learning process is assessed by the reward function $r^{\{t'\}}: \mathcal{S} \times \mathcal{A} \to \mathbb{R}$, which evaluates the effectiveness of state-action pairs [41]. Fig. 2 shows the MDP formulation in the STAR-RIS system with a DRL-based learning agent. Here, the learning agent (deployed in the BS) takes the state $s^{\{t'\}}$ as input. It then generates the action $a^{\{t'\}}$, which determines the phase shift of the STAR-RIS and the subsurface assignment variable. The action predicted for the time step t' can be expressed as $\mathbf{a}^{\{t'\}} = [\boldsymbol{\psi}^{\{t'\}}, \bar{\boldsymbol{\alpha}}^{\{t'\}}]$. The actions $\psi^{\{t'\}}$ are formulated using 3. The action corresponding to the subsurface assignment is $\bar{\alpha}^{\{t'\}} \in \mathbb{R}^N$. The n^{th} value of $\bar{\alpha}^{\{t'\}}$ is mapped appropriately to represent which user the n^{th} element of the STAR-RIS is allocated to, resulting in the subsurface assignment matrix A given in 4. The actions predicted by the model guide the transmission of signals from the BS to the DUs at the time step t'. The resulting SINR at the DUs in both the reflection and transmission spaces, given by $\gamma^{\{t'\}}$ (recall $\gamma^{\{t'\}} = \left[\gamma_r^{\{t'\}}, \gamma_t^{\{t'\}}\right]$), indicate the effectiveness of the chosen actions. These SINRs become part of the observation and contribute to the state representation

 $\mathbf{s}^{\{t'+1\}}$ for the next iteration of the learning agent where $\mathbf{s}^{\{t'+1\}} = \left[\boldsymbol{\gamma}_r^{\{t'\}}, \boldsymbol{\gamma}_t^{\{t'\}}, \boldsymbol{\psi}^{\{t'\}}, \bar{\boldsymbol{\alpha}}^{\{t'\}} \right]$. The reward is calculated as the average data rate of all DUs in the reflection and transmission spaces. The data rate at time step t' for DU k in the reflection space is given by $r_k^{r\{t'\}} = \log_2(1 + \gamma_k^{r\{t'\}})$; and for DU k in the transmission is given by $r_k^{t\{t'\}} = \log_2(1 + \gamma_k^{t\{t'\}})$. The reward at time step k' can be expressed as

$$r^{\{t'\}} = \frac{1}{K+L} \left(\sum_{k=1}^{K} r_k^{r\{t'\}} + \sum_{l=1}^{L} r_l^{t\{t'\}} \right). \tag{17}$$

In our work, we also propose to selectively deactivate a portion of the STAR-RIS elements by using an appropriate reward function for the proposed DRL solution, given by

$$r^{\{t'\}} = \frac{1}{K+L} \left(\sum_{k=1}^{K} r_k^{r\{t'\}} + \sum_{l=1}^{L} r_l^{t\{t'\}} \right) + \frac{\mu}{\sum_{n=1}^{N} \left(\sum_{k=1}^{K} \alpha_{kn}^{r\{t'\}} + \sum_{l=1}^{L} \alpha_{ln}^{t\{t'\}} \right)}.$$
 (18)

The first term represents the average data rate for all DUs at time step t'. The second term is added as a penalty based on the total number of activated STAR-RIS elements in the system with μ as a regularization parameter. The denominator of the second term represents the total number of activated STAR-RIS elements that are assigned to the DUs at time t'. The penalty term in the reward function helps to manage the trade-off between DU fairness and excessive use of STAR-RIS elements. The goal of the RL agent is to learn a policy, denoted $\pi: \mathcal{S} \to \mathcal{A}$, to maximize the expected cumulative return, $\mathbb{E}[\mathbb{F}^{\{t'\}}(\eta)|\pi]$, by considering the discounted rewards obtained at each time step t'. Here, η denotes the discounting factor ($\eta \in [0,1]$) and $\mathbb{F}^{\{t'\}}$ represents the return (or total discounted reward) starting from the time step t'. The return in time t' is given by $\mathbb{F}^{\{t'\}}(\eta) = \sum_{\hat{t}=t'}^{\infty} \eta^{\hat{t}-t'} r^{\{t'\}} (\mathbf{a}^{\{t'\}}, \mathbf{s}^{\{t'\}})$.

The DRL agent is trained using an actor-critic method, namely, the deep deterministic policy gradient (DDPG) [42]. The actor-critic algorithm is effective for solving non-convex combinatorial optimization problems by leveraging an actor network to learn a stochastic policy that selects optimal STAR-RIS phase-shift configurations along with subsurface assignment variables, while the critic network estimates the corresponding Q function to provide policy gradient updates. This framework facilitates efficient and adaptive optimization in high-dimensional hybrid discrete-continuous action spaces of the STAR-RIS. The DDPG algorithm simultaneously learns the Q function together with the policy. It uses the Bellman equation to learn the Q function, which is then utilized to optimize the policy. It contains four neural networks, namely, the actor network, critic network, target actor network, and target critic network. The actor network Π , which is parameterized by θ^a , takes the current state $\mathbf{s}^{\{t'\}}$ of

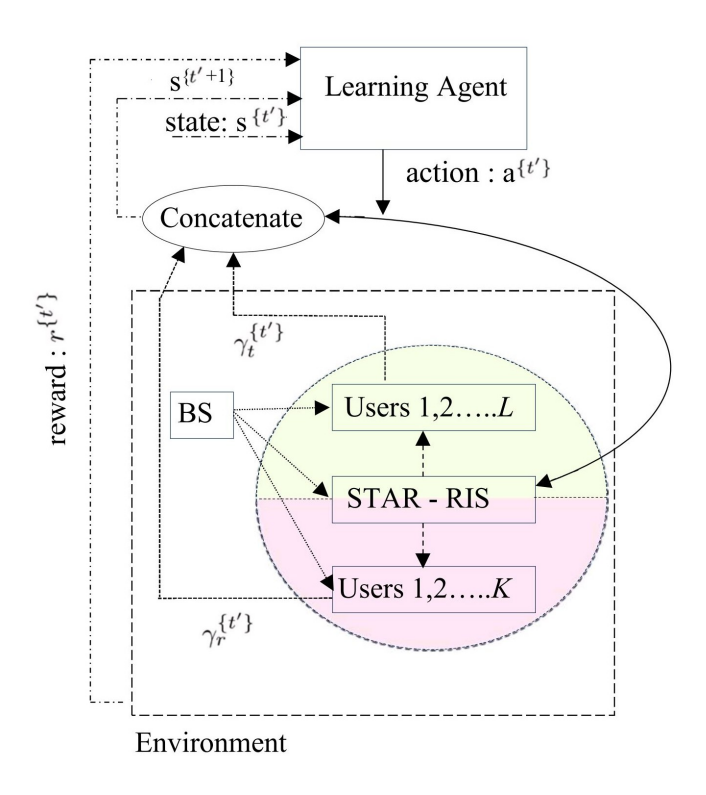


Fig. 2: MDP formulation in STAR-RIS system with DRL-based learning agent.

the environment as input and produces the corresponding action $\mathbf{a}^{\{t'\}}$ as output. On the other hand, the critic network Δ , which is parameterized by θ^c , takes both the state and the action as input and produces an output value that evaluates the effectiveness of the current policy [42]. In our case, the critic network is a fully connected network that gives a scalar output as Q-value. Two target networks were used to make learning more stable. The target actor network is parameterized by $\tilde{\theta}^{\mathbf{a}}$, and the target critic network is parameterized by $\tilde{\theta}^{\mathbf{c}}$. The environment gives the reward $r^{\{t'\}}$ after each action. At each training time step t', the current state $\mathbf{s}^{\{i\}}$, the executed action $\mathbf{a}^{\{i\}}$, the obtained reward $r^{\{i\}}$, and the subsequent state $\mathbf{s}^{\{i+1\}}$ are recorded as an experience $(\mathbf{s}^{\{i\}}, \mathbf{a}^{\{i\}}, r^{\{i\}}, \mathbf{s}^{\{i+1\}})$ in buffer B [42]. To train neural networks, \tilde{N} samples are taken from B. This is used to compute the gradients. The loss function is given by the mean squared Bellman error as shown below

$$\hat{L} = \frac{1}{\tilde{N}} \sum_{i=1}^{\tilde{N}} (\hat{y}^{\{i\}} - \Delta ((\mathbf{s}^{\{i\}}, \mathbf{a}^{\{i\}} \mid \theta^c))^2,$$
(19)

where $\Delta(\mathbf{s}^{\{i\}}, \mathbf{a}^{\{i\}} \mid \theta^c)$ represents the predicted output value of the critic network and $\hat{y}^{\{i\}}$

denotes the predicted return which is given by

$$\hat{y}^{\{i\}} = r^{\{i\}} + \eta \Delta \left(\mathbf{s}^{\{i+1\}}, \Pi(\mathbf{s}^{\{i+1\}} \mid \tilde{\theta}^a) \mid \tilde{\theta}^c \right). \tag{20}$$

The parameters of the actor and critic networks are updated based on $\theta^a \leftarrow \theta^a + \eta_a \frac{1}{\tilde{N}} \sum_{i=1}^{\tilde{N}} \left(\nabla_{\theta^a} \Pi(s) \nabla_a \Delta(s,a) \mid_{a=\Pi(s)} \right)$ and $\theta^c \leftarrow \theta^c - \eta_c \nabla_{\theta^c} \hat{L}$, where $\eta_a, \eta_c \ll 1$ denotes the step size for the stochastic update. In addition, DDPG agents update their target actor and critic parameters using $\tilde{\theta}^a \leftarrow \tilde{\lambda} \tilde{\theta}^a + (1-\tilde{\lambda}) \tilde{\theta}^a$ and $\tilde{\theta}^c \leftarrow \tilde{\lambda} \tilde{\theta}^c + (1-\tilde{\lambda}) \tilde{\theta}^c$ with $\tilde{\lambda} \ll 1$. Also note that we add Gaussian noise to the predicted action for better exploration in the action space and, therefore, faster convergence.

A. Key innovations in the DDPG algorithm:

The DDPG algorithm deals with continuous action and continuous state space. Our work addresses a pseudo-discrete action space where the STAR-RIS phase shift is continuous while the subsurface assignment variable is discrete. Deep Q-Networks, which are suitable for handling discrete action spaces, cannot be applied directly to handle a mixed action space like ours [43]. We use a two-part neural network to address the huge action space involving the STAR-RIS phase shift and the subsurface assignment variable. The first part, a feed-forward feature extractor (FE) with linear layers \tilde{L} using ReLU as an activation function and layer normalization, feeds its output to the second part, comprising two sub-networks (SN) that determine phase shifts and the subsurface assignment variable [25]. At time step t', the input to the FE is the state $\mathbf{u}_0 = \mathbf{s}^{\{t'\}}$. Each layer in FE is represented by weights $\mathbf{W}_l \in \mathbb{R}^{d_o^l \times d_i^l}$ and biases $\mathbf{b}_l \in \mathbb{R}^{d_o^l}$, where $l = 1, 2 \dots \tilde{L}$, denotes the layer index and d_o^l is the output dimension, and d_i^l is the input dimension. The output of FE $(\mathbf{u}_l \in \mathbb{R}^{d_o^l})$ is given by \mathbf{u}_l =ReLU $(\mathbf{W}_l\mathbf{u}_{l-1} + \mathbf{b}_l)$. The final output of the FE \mathbf{u}_L is then fed to the SNs. The first SN predicts the STAR-RIS phases with parameters $\mathbf{W}_{\psi} \in \mathbb{R}^{N imes d_o^l}$ and biases $\mathbf{b}_{\psi} \in \mathbb{R}^{N}$. We have $\mathbf{a}_{\psi} = \tanh(\mathbf{W}_{\psi}\mathbf{u}_{L} + \mathbf{b}_{\psi})$. Similarly, the second SN predicts the subsurface assignment variable with parameters $\mathbf{W}_{\bar{\alpha}} \in \mathbb{R}^{N \times d_o^l}$ and biases $\mathbf{b}_{\bar{\alpha}} \in \mathbb{R}^N$. We have $\mathbf{a}_{\bar{\alpha}}$ =tanh $(\mathbf{W}_{\bar{\alpha}}\mathbf{u}_L+\mathbf{b}_{\bar{\alpha}})$. It should be noted that in the DRL algorithm, the initial predicted continuous actions follow a Gaussian distribution with mean zero and unit standard deviation [25]. This makes it a challenge for the DRL to predict actions that lack symmetry. So, it is essential to normalize the actions using the hyperbolic tangent (tanh) activation function at the final layer of each SN. This normalization ensures that the actions are symmetric and confined within the range of [-1, +1]. Later, we adjust the output according to domain-specific knowledge of the

STAR-RIS phases and subsurface assignment variables by shifting and scaling. The STAR-RIS phase shifts are obtained by shifting and scaling the corresponding actions to ensure that they lie within the range $[0, 2\pi]$ before using it in the environment, therefore $\psi = 2\pi \times (\mathbf{a}_{\psi} + 1)/2$ radians. The subsurface assignment variable $\bar{\alpha}$ is a continuous vector output of the DRL policy, where each element corresponds to a specific STAR-RIS element and lies within the range [-1,1]. Since each STAR-RIS element must be assigned to at most one of the J=K+L DUs, the range [-1,1] is divided into equal intervals J, where each interval corresponds to a unique DU. To form the subsurface assignment matrix A, a discretization process is applied to map the continuous values of $\bar{\alpha}$ to binary assignments. Specifically, each STAR-RIS element n is assigned to the DU j based on the interval in which its corresponding action value $\bar{\alpha}_n$ (i.e., the *n*-th entry of $\bar{\alpha}$) falls. This results in a binary matrix $\mathbf{A} \in \{0,1\}^{J \times N}$, where $\mathbf{A}_{j,n} = 1$ indicates that element n is assigned to DU j, and all other entries in column n are 0 to ensure a unique assignment. Furthermore, in our work, we can selectively deactivate some of the STAR-RIS elements to improve resource utilization. To allow deactivation of STAR-RIS elements, actions corresponding to the subsurface assignment variables in the range [-1, 1] are uniformly divided into J+1 bins, where J bins correspond to DU assignments and one bin is reserved for element deactivation. We use the reward function given in (18) to enhance SINR performance while penalizing the use of excessive STAR-RIS elements.

B. Computational requirement of the proposed algorithm

In our simulations, we have considered three users in the reflection space and three users in the transmission space. Recall that (cf. Section III) to address the huge action space involving the STAR-RIS phase shift and subsurface assignment variable, we consider a two-part neural network, with a feed-forward FE and two SNs. At time t', the FE processes the state $\mathbf{u}_0 = \mathbf{s}^{\{t'\}}$, with dimension 6 + 2N. The first entry corresponds to the observed SINR values (resulting SINR in the DUs in both the transmission $(\gamma_t^{\{t'-1\}})$ and the reflection spaces $(\gamma_r^{\{t'-1\}})$) at time (t'-1). The next 2N entries correspond to the phase shift and the subsurface assignment variable of STAR-RIS, respectively. Assume that each two-layer FE layer has T neurons. The total floating-point operation performed at the FE is $2((6+2N)T+T^2)$. The floating-point operation for the first and second SNs is 2TN.

IV. PROPOSED HYBRID DEEP REINFORCEMENT LEARNING APPROACH

The specific MINLP problem given in \mathcal{P}_1 in Eq. (11) involving the optimization of the continuous STAR-RIS phase shifts and the binary subsurface assignment variable has not yet been addressed by any existing work regarding STAR-RIS [24], [37]–[40]. So, we have been further motivated to propose a hybrid approach in which the STAR-RIS phase shifts are optimized using a conventional scheme such as the Dinkelbach algorithm [44], and binary subsurface assignment variables are optimized using the DRL method. The motivation behind choosing Dinkelbach to solve for STAR-RIS phase shifts is that it solves optimization problems that are in fractional form, similar to ours. We compare the hybrid DRL with the proposed DRL method, which jointly optimizes both components. The proposed hybrid DRL is one of our key contributions, providing an intermediate step between fully conventional and fully learning-based solutions.

1) Phase shift optimization via Dinkelbach algorithm: We aim to solve for the phase shift of the STAR-RIS ψ , where the objective is to maximize the sum of the data rates of all DUs in both the reflection and transmission space. The resulting optimization problem is given by

$$\max_{\psi} \sum_{k=1}^{K} \log_2 (1 + \gamma_k^r) + \sum_{l=1}^{L} \log_2 (1 + \gamma_l^t)$$
s. t. $0 \le \theta_n^{\{r,t\}} \le 2\pi \quad \forall n \in 1, 2, \dots, N.$ (21)

In the above objective, max can be moved inside \log , because $\log(1+x)$ is strictly increasing and the optimization is carried out independently for each DU. The above phase optimization problem involves a fractional objective function, where the SINR for each DU is expressed as a quadratic ratios. To solve the non-convex optimization problem, we express the objective as a general fractional quadratic program, written as:

$$\max_{\mathbf{x} \in \mathcal{X}} \quad \frac{\mathbf{x}^T \mathbf{Q} \mathbf{x} + \mathbf{c}^T \mathbf{x} + d}{\mathbf{x}^T \mathbf{R} \mathbf{x} + \mathbf{b}^T \mathbf{x} + e}$$
(22)

where $\mathbf{c}, \mathbf{b} \in \mathbb{R}^n$, $\mathbf{Q}, \mathbf{R} \in \mathbb{R}^{n \times n}$ are symmetric matrices, and $d, e \in \mathbb{R}$ [45]. The set $\mathcal{X} \subseteq \mathbb{R}^n$ is assumed to be convex. We then apply the matrix lifting technique to relax the quadratic form into a convex semidefinite program (SDP) and then apply the Dinkelbach algorithm to iteratively handle the fractional structure [46], [47].

Let us first consider the reflection space alone. The formulation below can also be extended to the transmission space, leading to joint optimization over both domains. The signal term in the numerator of γ_k^r can be written as $\rho_t \left\| \mathbf{g}_k^r \tilde{\mathbf{\Theta}}_k^r \mathbf{G} \mathbf{w}_k + \mathbf{h}_k^r \mathbf{w}_k \right\|^2 = \rho_t \left((\tilde{s}_k^r)^H \operatorname{diag}(\mathbf{g}_k^r) \mathbf{G} \mathbf{w}_k + \mathbf{h}_k^r \mathbf{w}_k \right) \left((\tilde{s}_k^r)^H \operatorname{diag}(\mathbf{g}_k^r) \mathbf{G} \mathbf{w}_k + \mathbf{h}_k^r \mathbf{w}_k \right)^H$. Here, $\tilde{\mathbf{s}}_k^r$ is an N dimensional

vector that represents the STAR-RIS phase shift vector after incorporating the subsurface assignment variables in the reflection space (recall 2). Note that, $\tilde{\mathbf{s}}_k^r$ has non-zero entries only at the positions where $\alpha_{kn}^r = 1 \ \forall n \in 1, \dots, N$. Now, the augmented phase vector can be written as $\hat{\mathbf{s}}_k^r = \begin{bmatrix} \tilde{\mathbf{s}}_k^r \\ 1 \end{bmatrix} \in \mathbb{C}^{(N+1)\times 1}$. The lifted matrix is $\mathbf{V}_k = \hat{\mathbf{s}}_k^r \left(\hat{\mathbf{s}}_k^r\right)^H \in \mathbb{C}^{(N+1)\times (N+1)}$. Now, the numerator of γ_k^r is expressed as $\rho_t \|\mathbf{g}_k^r \tilde{\mathbf{\Theta}}_k^r \mathbf{G} \mathbf{w}_k + \mathbf{h}_k^r \mathbf{w}_k\|^2 = \rho_t \operatorname{Tr}(\tilde{\mathbf{Q}}_k \mathbf{V}_k)$, where

$$\widetilde{\mathbf{Q}}_k = egin{bmatrix} \mathbf{Q}_k & \mathbf{c}_k \\ \mathbf{c}_k^H & d_k \end{bmatrix}.$$

Here, $\mathbf{Q}_k = (\operatorname{diag}(\mathbf{g}_k^r)\mathbf{G}\mathbf{w}_k) (\operatorname{diag}(\mathbf{g}_k^r)\mathbf{G}\mathbf{w}_k)^H \in \mathbb{C}^{N\times N}$, $\mathbf{c}_k = (\operatorname{diag}(\mathbf{g}_k^r)\mathbf{G}\mathbf{w}_k) (\mathbf{h}_k^r\mathbf{w}_k)^H \in \mathbb{C}^{N\times 1}$, $d_k = (\mathbf{h}_k^r\mathbf{w}_k) (\mathbf{h}_k^r\mathbf{w}_k)^H \in \mathbb{R}$. Similarly, the denominator of γ_k^r becomes $\rho_t \operatorname{Tr}(\widetilde{\mathbf{R}}_k \mathbf{V}_k) + \sigma_k^2$, where $\widetilde{\mathbf{R}}_k \in \mathbb{C}^{(N+1)\times (N+1)}$ is defined as

$$\widetilde{\mathbf{R}}_k = egin{bmatrix} \mathbf{R}_k & \mathbf{b}_k \ \mathbf{b}_k^H & e_k \end{bmatrix}.$$

Here, $\mathbf{R}_k = \sum_{j \neq k} (\operatorname{diag}(\mathbf{g}_k^r) \mathbf{G} \mathbf{w}_j) (\operatorname{diag}(\mathbf{g}_k^r) \mathbf{G} \mathbf{w}_j)^H \in \mathbb{C}^{N \times N}$, $\mathbf{b}_k = \sum_{j \neq k} (\operatorname{diag}(\mathbf{g}_k^r) \mathbf{G} \mathbf{w}_j) (\mathbf{h}_k^r \mathbf{w}_j)^H \in \mathbb{C}^{N \times 1}$, $e_k = \sum_{j \neq k} (\mathbf{h}_k^r \mathbf{w}_j) (\mathbf{h}_k^r \mathbf{w}_j)^H \in \mathbb{R}$. Note that $\widetilde{\mathbf{Q}}_k, \widetilde{\mathbf{R}}_k \in \mathbb{C}^{(N+1) \times (N+1)}$ are Hermitian positive semidefinite matrices formed from the beamformers and channel matrices. By relaxing the rank constraint rank $(\mathbf{V}_k) = 1$, we obtain a convex SDP and solve it using the Dinkelbach algorithm [44]. The maximization problem for the k-th reflection DU is:

$$\max_{\mathbf{V}_{k} \succeq 0, \, [\mathbf{V}_{k}]_{N+1,N+1}=1} \frac{\rho_{t} \operatorname{Tr}(\widetilde{\mathbf{Q}}_{k} \mathbf{V}_{k})}{\rho_{t} \operatorname{Tr}(\widetilde{\mathbf{R}}_{k} \mathbf{V}_{k}) + \sigma_{k}^{2}}.$$
(23)

This is a non-convex problem due to the fractional structure inside the logarithm. To solve it efficiently, we apply the Dinkelbach algorithm. At each iteration t, for current values of $\hat{\lambda}_k^{(t)}$, we solve the following convex subproblem:

$$\max_{\substack{\mathbf{V}_k \succeq 0, \\ [\mathbf{V}_k]_{N+1,N+1} = 1}} \left(\rho_t \operatorname{Tr}(\widetilde{\mathbf{Q}}_k \mathbf{V}_k) - \hat{\lambda}_k^{(t)} (\rho_t \operatorname{Tr}(\widetilde{\mathbf{R}}_k \mathbf{V}_k) + \sigma_k^2) \right).$$

Each $\hat{\lambda}_k$ is updated iteratively as:

$$\hat{\lambda}_k^{(t+1)} = \frac{\rho_t \operatorname{Tr}(\widetilde{\mathbf{Q}}_k \mathbf{V}_k^{(t)})}{\rho_t \operatorname{Tr}(\widetilde{\mathbf{R}}_k \mathbf{V}_k^{(t)}) + \sigma_k^2}.$$
(24)

The iteration continues until convergence, i.e., until the Dinkelbach residuals satisfy

$$\left| \rho_t \operatorname{Tr}(\widetilde{\mathbf{Q}}_k \mathbf{V}_k^{(t)}) - \hat{\lambda}_k^{(t)} (\rho_t \operatorname{Tr}(\widetilde{\mathbf{R}}_k \mathbf{V}_k^{(t)}) + \sigma_k^2) \right| \le \tilde{\epsilon}, \quad \forall k$$
 (25)

where $\tilde{\epsilon}$ is a small positive constant.

- 2) Subsurface assignment variable optimization via DRL: Once we optimize the STAR-RIS phase shifts using the Dinkelbach algorithm, we predict the subsurface assignment variables using a DRL agent. This leads to a two-stage hybrid optimization strategy. The hybrid optimization strategy follows the following sequence in every time step:
 - 1) The DRL agent predicts the subsurface allocation $\bar{\alpha}^{\{t'\}}$, based on the current state.
 - 2) At each time step t', the Dinkelbach algorithm optimizes the phase vector $\psi^{\{t'\}}$, using the subsurface assignment variable as input produced by the DRL agent.
 - 3) The resulting sum of the DU data rates is computed and used as a reward to update the DRL agent.

V. RESULTS AND DISCUSSION

In this section, we investigate the performance of the proposed method and provide a performance comparison. The STAR-RIS, BS, and DUs are placed in a three-dimensional system similar to [20], [48], [49]. The BS and the STAR-RIS are located at (0,0,0), and (48,20,3), respectively. We consider three DUs (DUs 1, 2, and 3) in the transmission space and three in the reflection space (DUs 4, 5, and 6), each considered to be in different locations relative to STAR-RIS to have varying channel conditions. DU 2 is closest to the STAR-RIS in transmission space, followed by DU 1 and DU 3. Similarly, DU 5 is closest to STAR-RIS in the reflection space, followed by DU 4 and DU 6. The channels between BS to STAR-RIS, STAR-RIS to DU, and BS to DU are modeled as Rician channels, as mentioned in Section II. Table II summarizes the key simulation and training parameters used in our experiments. At the beginning of every episode, i.e., in timestep t' = 0, the proposed DRL method randomly chooses actions, phase shifts $\psi^{\{0\}}$ from a uniform random distribution $U(0, 2\pi)$; $\bar{\alpha}^{\{0\}}$ from U(-1, 1).

A. Study the impact of subsurface assignment variable on achieving fair and high data rates among static DUs

In this subsection, we study how the subsurface assignment variable helps to achieve fair and high data among static DUs. We first look at a method where each DU is using the same number of STAR-RIS elements, and the DRL algorithm predicts only the STAR-RIS phase shifts.

1) Equal partitioning of STAR-RIS elements: Consider the scenario of N=36 ($N^t=N^r=18$) elements, where every DU uses a fixed number of six elements. The data rates (bps/Hz) of the DUs located near (DU 2 and DU 5) the STAR-RIS are high, and the data rate of the DUs far

TABLE II: Simulation and Training Parameters

System and Channel Parameters						
Rician factor (BS-STAR-RIS,	10 [33], [50]					
STAR-RIS-User)						
System bandwidth	100 MHz [51]					
Noise power density	-174 dBm/Hz [52]					
Carrier frequency f_c	3.5 GHz					
BS transmit power P_t	30 dBm					
Evaluation metric	DL data rate (bps/Hz)					
DRL Training Parameters						
Discount factor η	0.6					
Replay buffer size	10,000					
Actor learning rate	0.0001					
Critic learning rate	0.001					
Number of episodes	210					
Time steps per episode	1000					
Independent runs (averaged)	4					
Hardware used	NVIDIA GeForce RTX 2080 Ti GPU					

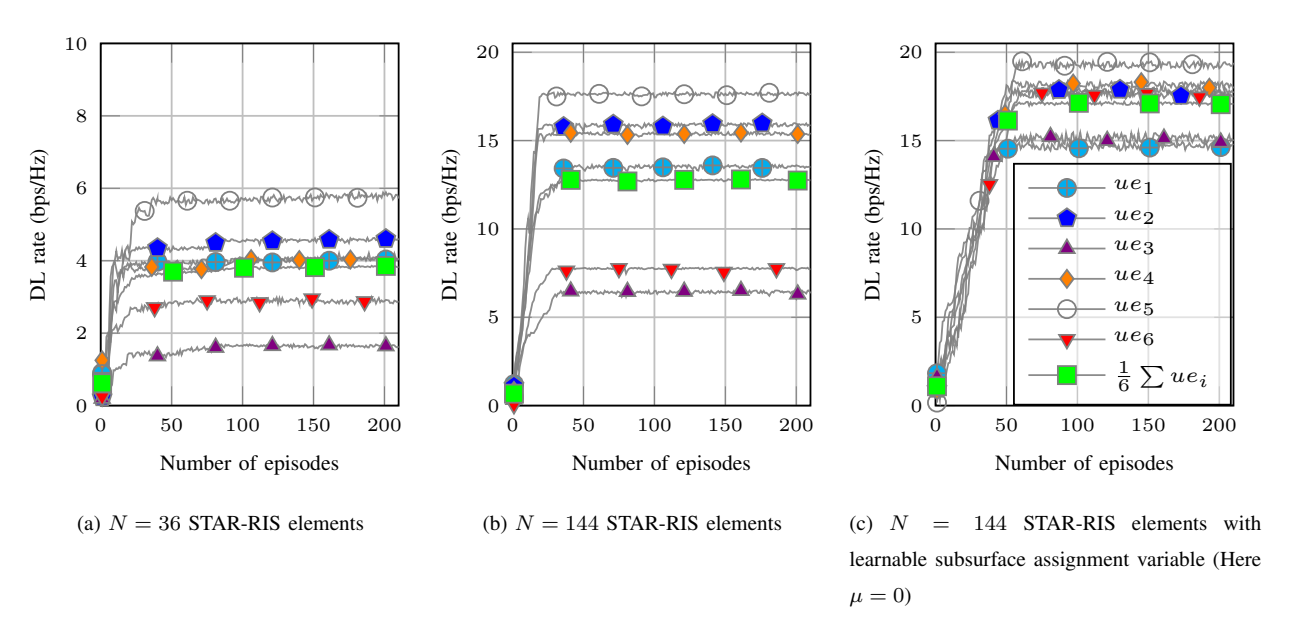
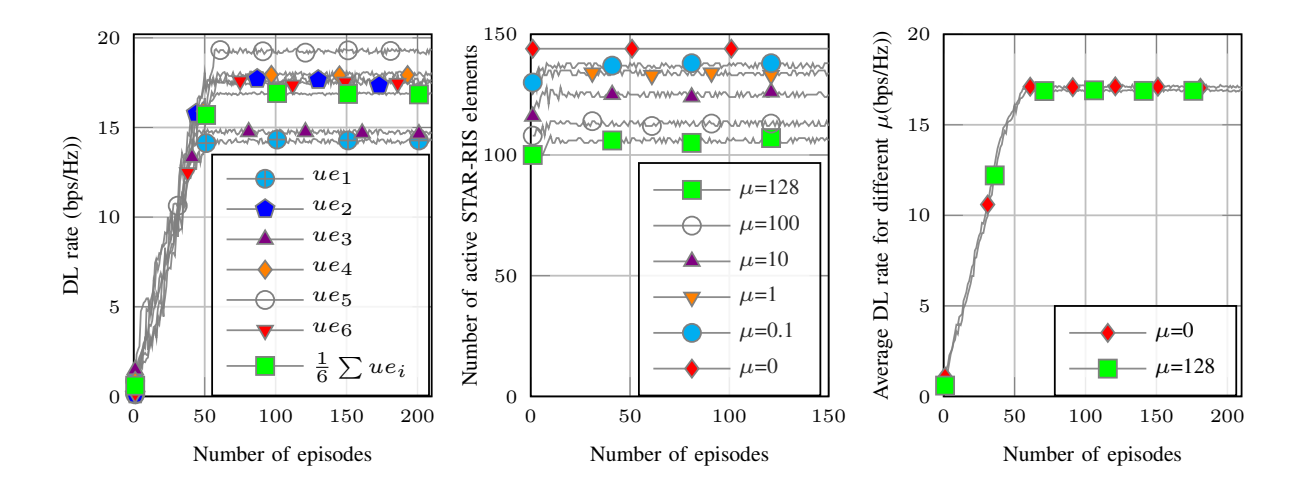


Fig. 3: The effect of increasing the number of STAR-RIS elements is shown in (a) and (b), where the elements are equally partitioned between the DUs irrespective of their location and channel condition. The DL rate for the k-th DU is represented with ue_k . The average DL rate $(\frac{1}{6} \sum ue_i)$ improves when STAR-RIS elements are partitioned based on the learnable subsurface assignment variable, as shown in (c). The legends are shared across the subfigures.

(DU 3 and DU 6) from the STAR-RIS is low, as shown in Fig. 3a. Therefore, equal partitioning of the elements leads to poor data rates for DUs located far from the STAR-RIS and is not fair.

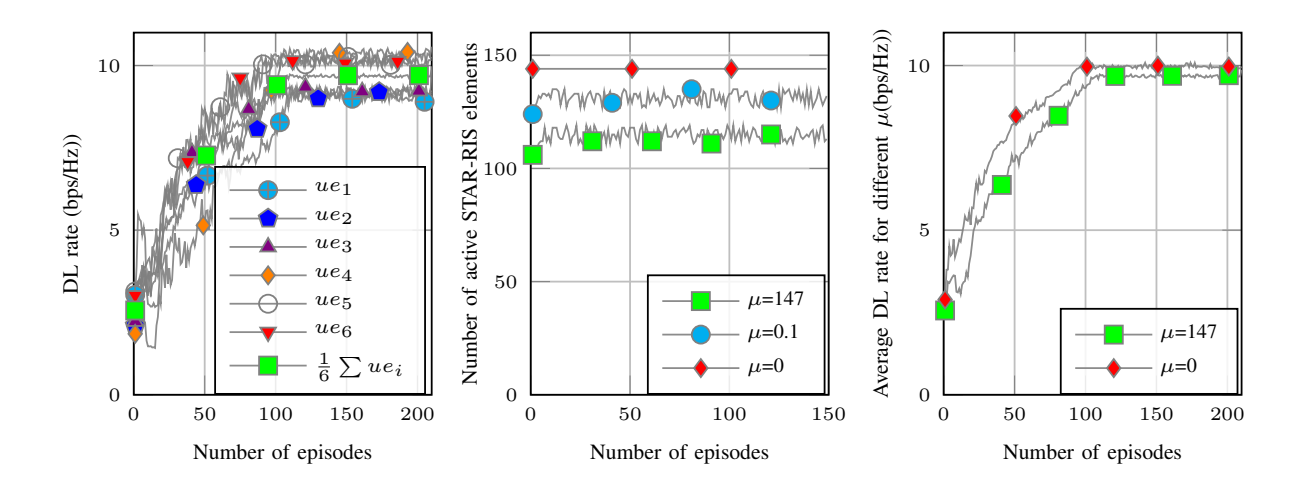


- (a) N = 144 STAR-RIS elements with y = 128
- (b) N=144 STAR-RIS elements with (c) N=144 STAR-RIS elements (μ values varying μ values = 0 and 128)

Fig. 4: The effect of shutting down the elements of STAR-RIS in a static DU scenario: (a) Data rate plot (better visible in colour) (b) Number of active STAR-RIS elements for different μ values vs. number of episodes, and (c) Average data rate vs. number of episodes for different μ values. Notably, the average data rate remains nearly constant for μ values of 0 and 128

We now examine the effect of increasing the STAR-RIS elements under equal partitioning. With an increased number of STAR-RIS elements, i.e., N=144 ($N^t=N^r=72$) each DU is served by 24 elements. From Fig. 3b, it can be seen that the average data rate of the system increases. The DL data rates of distant DUs also increase at a much higher rate. So, this scale-up effect indicates that increasing the number of STAR-RIS elements increases the average data rate and improves communication performance for all DUs. This also shows that the performance of distant users with poor channel conditions can be improved by increasing the number of STAR-RIS elements dedicated to them, which motivates us to use a varying number of STAR-RIS elements based on the channel condition of each DU.

2) Proposed DRL-based joint optimization of subsurface assignment variable and STAR-RIS phase shift: Instead of an equal number of STAR-RIS elements per DU, the proposed DRL method learns to predict A (4) for all DUs based on the channel condition. We consider N=144 ($N^t=N^r=72$) STAR-RIS elements. The reward function given by Eq. 18 is equivalent to Eq. 17 for $\mu=0$, and with this reward function, none of the STAR-RIS elements are deactivated. To ensure that the constraints 11c and 11d hold, i.e., each user is served by at least one element, we fix at least one element for each DU, and the assignment of the rest of the elements is predicted



- (a) N=144 STAR-RIS elements with $\mu=147$
- (b) N=144 STAR-RIS elements with (c) N=144 STAR-RIS elements (μ values varying μ values =0 and 147)

Fig. 5: The effect of shutting down the elements of STAR-RIS in a mobile DU scenario: (a) Data rate plot (better visible in colour) (b) Number of active STAR-RIS elements for different μ values vs. number of episodes, and (c) Average data rate vs. number of episodes for different μ values. Even in dynamic scenarios, the average data rate remains similar for μ values of 0 and 147. The observed fluctuations in the graphs are due to the dynamic nature of the scenario, where the phase-shift and subsurface assignment variables of the STAR-RIS are continuously optimized using DRL.

by the DRL algorithm.

In Fig. 3c, it can be observed that the predicting subsurface assignment matrix using the proposed DRL method improves average data rates, mainly benefiting DU 3 and DU 6, spatially distant from STAR-RIS without any degradation of the data rates of the other DUs. The proposed method can be compared with the equal partitioning given in Fig. 3c and Fig. 3b, respectively, where it is interesting to note that the use of more STAR-RIS elements for DUs is not always beneficial. As the method intelligently allocates more elements to distant DUs with a poorer channel condition, DUs with comparatively better channel conditions are left with a smaller number of elements. Even with a smaller number of STAR-RIS elements, the data rates of these DUs (DU 5, DU 2, DU 4, and DU 1) improve. The average data rate increases by 36% compared to the equal partitioning. So, given that we have more than enough STAR-RIS elements than what is needed to serve all the DUs, it will be of great interest to see if we can selectively deactivate some of the STAR-RIS elements to achieve similar performance to make the system more resource efficient.

3) Selectively deactivating STAR-RIS elements: We also investigate the effect of deactivating some of the STAR-RIS elements, where we have N=144 ($N^t=N^r=72$) STAR-RIS elements. Using a value of $\mu=128$ in (18), we penalize the use of excess STAR-RIS elements and plot the data rates of all DUs and the average data rate in Fig. 4a. We obtain a similar average data rate for both $\mu=0$ and $\mu=128$ as shown in Figs. 3c and 4a, respectively. We are also interested in looking at the number of active STAR-RIS elements for different values of μ .

Fig. 4b shows the total number of active STAR-RIS elements per episode for different μ . A comparatively higher value of μ forces the DRL agent to selectively deactivate more STAR-RIS elements. For $\mu=0$, all the elements of STAR-RIS are active. For values of μ ranging from 0.1 to 128, the number of active elements decreases from 136 to 105, indicating that the DRL model effectively deactivates elements. With $\mu=128$, we can deactivate almost 27% of the STAR-RIS elements (active elements reduced from 144 to 105), thus improving resource utilization. Fig. 4c shows the plot between the average data rate vs. the number of episodes for $\mu=0$ and $\mu=128$. As the proposed method can deactivate almost 27% of the STAR-RIS elements, without any compromise on data rate, we validate that the proposed method improves resource utilization without sacrificing overall system performance.

In a scenario with mobile DUs, the channel condition of the DUs keeps changing as they move, and the system becomes highly dynamic and non-stationary. Solving such a problem with the traditional approach may be computationally involved and time-consuming. However, the proposed DRL method can dynamically predict the number of STAR-RIS elements for each DU based on their channel conditions.

B. Study the impact of subsurface assignment variable on achieving fair and high data rates among mobile DUs:

We now evaluate the effectiveness of the proposed method for mobile DUs, using the Random Waypoint (RWP) mobility model. This model is widely used due to its simplicity, ease of implementation, and ability to represent unrestricted mobility patterns [53]. In this model, the movement of the entity is characterized by random changes in position and orientation. The DUs move in a total square area of 100m^2 with an average speed of 1m per time step, and at the beginning of each episode, the DU positions are randomly initialized [25]. Each time step corresponds to 1s. As DUs move, channel conditions become dynamic and lead to a Doppler shift in the channel (recall 14, 15, and 16). Here, we consider the scenario of N = 144 STAR-RIS

elements. The average data rate of the mobile DUs for each episode is plotted in Fig. 5a. It can be seen that, even though our channels are dynamically changing, we still achieve fair and high data rates for all DUs.

Fig. 5b illustrates the plot between the total number of active STAR-RIS elements per episode for different values of μ . In this, we examine the cases of $\mu=0.1$ and $\mu=147$. Due to user mobility, the number of elements allocated to DUs changes over time, resulting in a fluctuating plot over the episodes. With $\mu=0.1$, an average of 131 elements actively serve the DUs. On the other hand, when $\mu=147$, the average number of activated elements decreases to 114. So, with our proposed model, we can deactivate almost 21% of elements on average, thereby improving the overall utilization of the resource of the STAR-RIS system. Fig. 5c shows the graph of the average data rate for training episodes for $\mu=0$ and $\mu=147$. It can be observed that even in a dynamic user scenario, the average data rate remains almost similar for both $\mu=0$ and $\mu=147$ because the DRL agent learns to deactivate the excess STAR-RIS elements without any degradation in data rates. Thus, our proposed model effectively utilizes DRL to ensure fair and high data rates for all DUs in reflection and transmission spaces, while improving the resource efficiency of the STAR-RIS.

C. Comparison of the proposed methods:

We compare the performance and the computational characteristics of our proposed methods for a multi-user static scenario. For this, we have taken N=36 STAR-RIS elements. We consider three DUs in the reflection space and three DUs in the transmission space. First, we compare the performance of the DRL method with the performance of the Dinkelbach algorithm to solve the STAR-RIS phase shifts alone.

- DRL-ZF-PS: Phase shifts optimized using DRL with ZF beamforming
- DRL-MRT-PS: Phase shifts optimized using DRL with MRT beamforming
- Dinkelbach-MRT-PS: Phase shifts optimized using the Dinkelbach algorithm with MRT Next, we have compared the proposed DRL method with the proposed hybrid DRL approach.
 - DRL-ZF: A proposed DRL-based method that jointly optimizes STAR-RIS phase shifts and subsurface assignment with ZF beamforming
 - DRL-MRT: A proposed DRL-based method that jointly optimizes STAR-RIS phase shifts and subsurface assignment with MRT beamforming

- Hybrid-DRL-MRT: A proposed hybrid approach where the Dinkelbach algorithm optimizes
 phase shifts, and DRL solves the subsurface assignment variable iteratively with MRT
 beamforming
- 1) Comparison of the DRL with Dinkelbach for phase shift optimization: In this section, we evaluate the performance of the DRL method, using both ZF and MRT beamforming separately and comparing them with a Dinkelbach-based iterative optimization algorithm, which uses MRT beamforming. For this method, we assume that the subsurface assignment variables are set to 1 for a fixed set of 6 STAR-RIS elements per DU, resulting in an equal partitioning of all N=36 elements among the 6 DUs. Fig. 6 shows the average DL data rates for the training episodes. We observe that the DRL-ZF-PS achieves a final average data rate of 3.8 bps/Hz, while its MRT counterpart DRL-MRT-PS reaches 2.8 bps/Hz. The Dinkelbach-MRT-PS rapidly converges within the first few episodes to 2.5 bps/Hz. DRL-ZF-PS achieves a 52% higher average data rate compared to Dinkelbach-MRT-PS. However, the main disadvantage of the Dinkelbach scheme is that this method is computationally intensive.
- 2) Comparison of the proposed DRL method with the hybrid approach: The proposed hybrid-DRL-MRT approach is seen to converge quickly, reaching an average data rate of 3.0 bps/Hz. However, this method introduces considerable computational overhead as it depends on solving convex optimization problems iteratively for a fixed number of iterations using CVXPY in each time step. To give an idea about the computational complexity involved, we give Table III, which shows the run-time during the inference while both are run on the same device (for 1 episode). The computational overhead increases further as we increase the number of STAR-RIS elements. The proposed hybrid DRL is one of our key contributions, providing an intermediate step between fully conventional and fully learning-based solutions. Even though the proposed DRL method achieves a higher average downlink data rate, the proposed hybrid DRL converges quickly and can be a practical choice in scenarios where sufficient compute power is available and slightly lower performance is acceptable. The proposed DRL-ZF achieves the highest overall performance among all the schemes, reaching approximately 4.4 bps/Hz, and the proposed DRL-MRT achieves approximately 3.3 bps/Hz after 40 episodes, as shown in Fig. 6. The DRL-ZF method has a performance 46% better than hybrid-DRL-MRT. The DRL-ZF also eliminates the need for convex optimization in each episode, resulting in faster inference compared to the hybrid DRL scheme. Moreover, the proposed DRL method adapts better to dynamic scenarios, making it suitable for environments with user mobility and rapidly changing

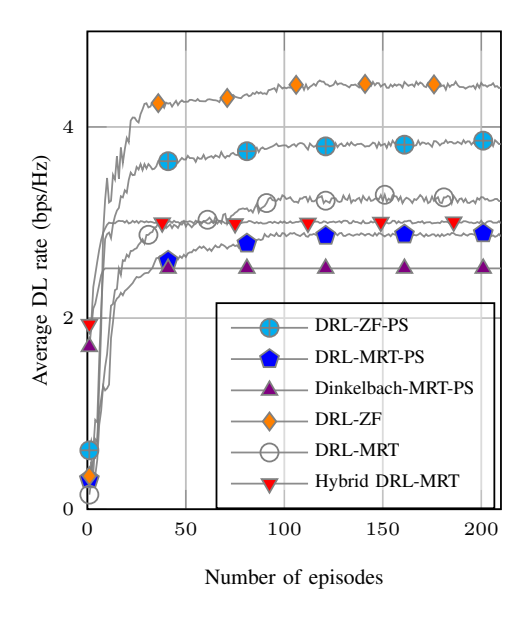


Fig. 6: Average DL data rate vs. number of episodes for various learning schemes

TABLE III: Computational complexity (evaluation time) comparison

Method	Steps per episode	Per step time (s)	Total time (s)
DRL-MRT	1000	0.0032	3.2
Hybrid DRL-MRT	1000	0.021	21

channel conditions.

VI. CONCLUSION

This work lays the foundation for utilizing the STAR-RIS elements efficiently to ensure fair data rates for static and mobile DUs. We formulated a novel optimization problem that maximizes the sum of the DU data rates and solved it using a DRL algorithm that jointly determines the allocation of STAR-RIS elements to different DUs and phase shifts of STAR-RIS, to give DUs fair data rates while maintaining efficient resource utilization. We first consider the effect of equal and unequal partitioning of the elements of STAR-RIS. Our results show that the average data rate increases by 36% while learning the subsurface assignment variables using the proposed DRL method compared to the equal partitioning with the same number of elements per DU in the static DU scenario. The learnable subsurface assignment variable helps to dynamically allocate the STAR-RIS elements to the DUs, even when the DUs move to get fair data rates across all the DUs. Furthermore, by using a regularized penalty term for the DRL agent, one

can selectively deactivate excess STAR-RIS elements, leading to efficient resource utilization of STAR-RIS elements. Our simulation results indicate that, on average, we can deactivate 27% of STAR-RIS elements in a static DU scenario and 21% of STAR-RIS elements in a moving DU scenario without any loss in performance. The proposed DRL method has been compared with a Dinkelbach algorithm and a designed hybrid DRL approach. The simulation results show that the proposed DRL achieves the highest average data rate among all.

REFERENCES

- [1] E. Basar, M. Di Renzo, J. De Rosny, M. Debbah, M.-S. Alouini, and R. Zhang, "Wireless communications through reconfigurable intelligent surfaces," *IEEE Access*, vol. 7, pp. 116753–116773, 2019.
- [2] Y. Liu, X. Mu, J. Xu, R. Schober, Y. Hao, H. V. Poor, and L. Hanzo, "STAR: Simultaneous transmission and reflection for 360° coverage by intelligent surfaces," *IEEE Wireless Commun.*, vol. 28, no. 6, pp. 102–109, 2021.
- [3] X. Mu, Y. Liu, L. Guo, J. Lin, and R. Schober, "Simultaneously transmitting and reflecting (STAR) RIS aided wireless communications," *IEEE Trans. Wireless Commun.*, vol. 21, no. 5, pp. 3083–3098, 2021.
- [4] J. Xu, Y. Liu, X. Mu, R. Schober, and H. V. Poor, "STAR-RISs: A correlated T&R phase-shift model and practical phase-shift configuration strategies," *IEEE J. Sel. Top. Signal Process.*, vol. 16, no. 5, pp. 1097–1111, 2022.
- [5] M. Ahmed, A. Wahid, S. S. Laique, W. U. Khan, A. Ihsan, F. Xu, S. Chatzinotas, and Z. Han, "A survey on STAR-RIS: Use cases, recent advances, and future research challenges," *IEEE Internet Things J.*, vol. 10, no. 16, pp. 14689–14711, 2023.
- [6] C. Wu, C. You, Y. Liu, S. Han, and M. D. Renzo, "Two-timescale design for STAR-RIS-aided NOMA systems," *IEEE Trans. Commun.*, vol. 72, no. 1, pp. 585–600, 2024.
- [7] J. Yaswanth, M. Katwe, K. Singh, O. Taghizadeh, C. Pan, and A. Schmeink, "Towards green communication: Power-efficient beamforming for STAR-RIS-aided SWIPT," *IEEE Trans. Green Commun. Netw.*, vol. 8, no. 4, pp. 1545–1563, 2024.
- [8] C. Wu, X. Mu, Y. Liu, X. Gu, and X. Wang, "Resource allocation in STAR-RIS-aided networks: OMA and NOMA," *IEEE Trans. Wireless Commun.*, vol. 21, no. 9, pp. 7653–7667, 2022.
- [9] K. Xie, G. Cai, G. Kaddoum, and J. He, "Performance analysis and resource allocation of STAR-RIS-aided wireless-powered NOMA system," *IEEE Trans. Commun.*, vol. 71, no. 10, pp. 5740–5755, 2023.
- [10] Q. Zhang, Y. Wang, H. Li, S. Hou, and Z. Song, "Resource allocation for energy efficient STAR-RIS aided MEC systems," IEEE Wireless Commun. Lett., vol. 12, no. 4, pp. 610–614, 2023.
- [11] M. Aldababsa, A. Khaleel, and E. Basar, "STAR-RIS-NOMA networks: An error performance perspective," *IEEE Commun. Lett.*, vol. 26, no. 8, pp. 1784–1788, 2022.
- [12] J. Zhao, Y. Zhu, X. Mu, K. Cai, Y. Liu, and L. Hanzo, "Simultaneously transmitting and reflecting reconfigurable intelligent surface (STAR-RIS) assisted UAV communications," *IEEE J. Sel. Areas Commun.*, vol. 40, no. 10, pp. 3041–3056, 2022.
- [13] T.-H. Vu, T.-V. Nguyen, Q.-V. Pham, D. B. da Costa, and S. Kim, "STAR-RIS-enabled short-packet NOMA systems," *IEEE Trans. Veh. Technol.*, vol. 72, no. 10, pp. 13764–13769, 2023.
- [14] M. Aldababsa, A. A. Mwais, and M. Obaid, "Performance of STAR-RIS assisted NOMA networks in Nakagami-m fading channels," *AEU-International Journal of Electronics and Communications*, vol. 166, p. 154685, 2023.
- [15] F. Karim, S. K. Singh, K. Singh, S. Prakriya, and C.-P. Li, "Performance analysis for RSMA-empowered STAR-RIS-aided downlink communications," in 2023 IEEE 34th Annual International Symposium on Personal, Indoor and Mobile Radio Communications (PIMRC). IEEE, 2023, pp. 1–6.

- [16] X. Luo, Z. Jiang, F. Xu, X. Li, G. Zhu, and K. Shen, "Sum-rate maximization for STAR-RIS-assisted multi-user networks with hardware impairments," *IEEE Wireless Commun. Lett.*, 2024.
- [17] M. V. Katwe, R. Deshpande, K. Singh, C. Pan, P. H. Ghare, and T. Q. Duong, "Spectrally-efficient beamforming design for STAR-RIS-aided URLLC NOMA systems," *IEEE Trans. Commun.*, vol. 72, no. 7, pp. 4414–4431, 2024.
- [18] C. Meng, K. Xiong, W. Chen, B. Gao, P. Fan, and K. B. Letaief, "Sum-rate maximization in STAR-RIS assisted RSMA networks: A PPO-based algorithm," *IEEE Internet Things J.*, 2023.
- [19] L. Wang, B. Ai, Y. Niu, Z. Zhong, Z. Han, and N. Wang, "Joint Reliability Optimization and Beamforming Design for STAR-RIS-Aided Multi-user MISO URLLC systems," *IEEE Trans. Veh. Technol.*, 2024.
- [20] Y. Eghbali, S. Faramarzi, S. K. Taskou, M. R. Mili, M. Rasti, and E. Hossain, "Beamforming for STAR-RIS-Aided Integrated Sensing and Communication Using Meta DRL," *IEEE Commun. Lett.*, 2024.
- [21] P. Shang, X. Han, J. Hou, J. Li, and S. Wang, "Enhanced Generalized Spatial Modulation for STAR-RIS-Aided Vehicular Communication System," *IEEE Trans. Consum. Electron.*, 2025.
- [22] Q. Wu and R. Zhang, "Intelligent reflecting surface enhanced wireless network via joint active and passive beamforming," *IEEE Trans. Wireless Commun.*, vol. 18, no. 11, pp. 5394–5409, 2019.
- [23] L. Xue, K. Wang, Z. Yang, and M. Peng, "Max-min energy-efficiency fair optimization in STAR-RIS assisted communication system," *IEEE Access*, vol. 11, pp. 51106–51116, 2023.
- [24] P. P. Perera, V. G. Warnasooriya, D. Kudathanthirige, and H. A. Suraweera, "Sum rate maximization in STAR-RIS assisted full-duplex communication systems," in *Proc. 2022 IEEE International Conference on Communications (ICC)*, 2022, pp. 3281–3286.
- [25] N. Nayak, S. Kalyani, and H. A. Suraweera, "A DRL approach for RIS-assisted full-duplex UL and DL transmission: Beamforming, phase shift and power optimization," *IEEE Trans. Wireless Commun.*, vol. 23, no. 10, pp. 14652–14666, 2024.
- [26] Z. Ma, Q. Zhao, B. Yan, and J. Zhang, "Deep reinforcement learning enabled joint deployment and beamforming in STAR-RIS assisted networks," *arXiv preprint arXiv:2309.03520*, 2023.
- [27] X. Gao, W. Yi, Y. Liu, J. Zhang, and P. Zhang, "DRL enabled coverage and capacity optimization in STAR-RIS-assisted networks," *IEEE Trans. Commun.*, no. 11, pp. 6616–6632, 2023.
- [28] Y. Hu, K. Kang, H. Zhu, X. Luo, and H. Qian, "Serving mobile users in intelligent reflecting surface assisted massive MIMO System," *IEEE Trans. Veh. Technol.*, vol. 71, no. 6, pp. 6384–6396, 2022.
- [29] Z. Huang, B. Zheng, and R. Zhang, "Transforming Fading Channel from Fast to Slow: IRS-Assisted High-Mobility Communication," in *Proc.* 2021 IEEE International Conference on Communications (ICC), 2021, pp. 1–6.
- [30] M. Eskandari, H. Zhu, A. Shojaeifard, and J. Wang, "Statistical CSI-Based Beamforming for RIS-Aided Multiuser MISO Systems via Deep Reinforcement Learning," *IEEE Wireless Commun. Lett.*, vol. 13, no. 2, pp. 570–574, 2023.
- [31] E. Björnson, H. Wymeersch, B. Matthiesen, P. Popovski, L. Sanguinetti, and E. De Carvalho, "Reconfigurable intelligent surfaces: A signal processing perspective with wireless applications," *IEEE Signal Process. Mag.*, vol. 39, no. 2, pp. 135–158, 2022.
- [32] U. Madhow, Fundamentals of digital communication. Cambridge university press, 2008.
- [33] K. Feng, Q. Wang, X. Li, and C.-K. Wen, "Deep reinforcement learning based intelligent reflecting surface optimization for MISO communication systems," *IEEE Wireless Commun. Lett.*, vol. 9, no. 5, pp. 745–749, 2020.
- [34] H. Chang, X. Kang, H. Lei, T. A. Tsiftsis, G. Pan, and H. Liu, "STAR-RIS-aided covert communications in MISO-RSMA systems," *IEEE Trans. Green Commun. Netw.*, 2024.
- [35] C. Liu, R. He, Y. Niu, S. Mao, B. Ai, and R. Chen, "Refracting Reconfigurable Intelligent Surface Assisted URLLC for Millimeter Wave High-Speed Train Communication Coverage Enhancement," *IEEE Trans. Veh. Technol.*, 2024.

- [36] T. S. Rappaport, Wireless communications: principles and practice. Cambridge University Press, 2024.
- [37] S. Zhang, S. Bao, K. Chi, K. Yu, and S. Mumtaz, "DRL-based computation rate maximization for wireless powered multi-AP edge computing," *IEEE Trans. Commun.*, 2023.
- [38] T. Zhang, P. Ren, D. Xu, and Z. Ren, "RIS subarray optimization with reinforcement learning for green symbiotic communications in Internet of Things," *IEEE Internet Things J.*, vol. 10, no. 22, pp. 19454–19465, 2023.
- [39] P. S. Aung, L. X. Nguyen, Y. K. Tun, Z. Han, and C. S. Hong, "Aerial STAR-RIS empowered MEC: A DRL approach for energy minimization," *IEEE Wireless Commun. Lett.*, vol. 13, no. 5, pp. 1409–1413, 2024.
- [40] R. Huang and V. W. Wong, "Joint user scheduling, phase shift control, and beamforming optimization in intelligent reflecting surface-aided systems," *IEEE Trans. Wireless Commun.*, vol. 21, no. 9, pp. 7521–7535, 2022.
- [41] V. Raj, N. Nayak, and S. Kalyani, "Deep reinforcement learning based blind mmWave MIMO beam alignment," *IEEE Trans. Wireless Commun.*, vol. 21, no. 10, pp. 8772–8785, 2022.
- [42] T. P. Lillicrap, J. J. Hunt, A. Pritzel, N. Heess, T. Erez, Y. Tassa, D. Silver, and D. Wierstra, "Continuous control with deep reinforcement learning," *arXiv preprint arXiv:1509.02971*, 2015.
- [43] V. Mnih, K. Kavukcuoglu, D. Silver, A. Graves, I. Antonoglou, D. Wierstra, and M. Riedmiller, "Playing atari with deep reinforcement learning," *arXiv preprint arXiv:1312.5602*, 2013.
- [44] A. Kafizov, A. Elzanaty, L. R. Varshney, and M.-S. Alouini, "Wireless network coding with intelligent reflecting surfaces," *IEEE Commun. Lett.*, vol. 25, no. 10, pp. 3427–3431, 2021.
- [45] H. Alwazani, A. Kammoun, A. Chaaban, M. Debbah, M.-S. Alouini et al., "Intelligent reflecting surface-assisted multi-user MISO communication: Channel estimation and beamforming design," IEEE Open J. Commun., vol. 1, pp. 661–680, 2020.
- [46] A. Zappone, L. Sanguinetti, G. Bacci, E. Jorswieck, and M. Debbah, "Energy-efficient power control: A look at 5G wireless technologies," *IEEE Trans. Signal Process.*, vol. 64, no. 7, pp. 1668–1683, 2015.
- [47] A. Subhash, A. Kammoun, A. Elzanaty, S. Kalyani, Y. H. Al-Badarneh, and M.-S. Alouini, "Max-min SINR optimization for RIS-aided uplink communications with green constraints," *IEEE Wireless Commun. Lett.*, vol. 12, no. 6, pp. 942–946, 2023.
- [48] W. Ni, Y. Liu, Y. C. Eldar, Z. Yang, and H. Tian, "STAR-RIS integrated nonorthogonal multiple access and over-the-air federated learning: Framework, analysis, and optimization," *IEEE Internet Things J.*, vol. 9, no. 18, pp. 17136–17156, 2022.
- [49] M. Umer, M. A. Mohsin, S. A. Hassan, H. Jung, and H. Pervaiz, "Performance analysis of STAR-RIS enhanced CoMP-NOMA multi-cell networks," in *Proc. 2023 IEEE Globecom Workshops (GC Wkshps)*, 2023, pp. 2000–2005.
- [50] C. Wu, C. You, Y. Liu, X. Gu, and Y. Cai, "Channel estimation for STAR-RIS-aided wireless communication," *IEEE Commun. Lett.*, vol. 26, no. 3, pp. 652–656, 2021.
- [51] A. Taha, Y. Zhang, F. B. Mismar, and A. Alkhateeb, "Deep reinforcement learning for intelligent reflecting surfaces: Towards standalone operation," in *Proc. IEEE 21st international workshop on signal processing advances in wireless communications (SPAWC 2020)*, 2020, pp. 1–5.
- [52] Z. Peng, Z. Zhang, C. Pan, L. Li, and A. L. Swindlehurst, "Multiuser full-duplex two-way communications via intelligent reflecting surface," *IEEE Trans. Signal Process.*, vol. 69, pp. 837–851, 2021.
- [53] D. B. Johnson and D. A. Maltz, "Dynamic source routing in ad hoc wireless networks," *Mobile Computing*, pp. 153–181, 1996.